



1 Only a minority of bacteria grow after wetting in both  
2 natural and post-mining biocrusts in a hyperarid,  
3 phosphate mine

4

5 Talia Gabay<sup>1,2</sup>, Eva Petrova<sup>3</sup>, Osnat Gillor<sup>2</sup>, Yaron Ziv<sup>1</sup>, and Roey Angel<sup>3\*</sup>

6

7 <sup>1</sup>Department of Life Sciences, Ben Gurion University of the Negev, 8410501, Israel

8 <sup>2</sup>Zuckerberg Institute for Water Research, Blaustein Institutes for Desert Research, Ben-Gurion

9 University of the Negev, 8499000, Israel

10 <sup>3</sup>Institute of Soil Biology and Biogeochemistry, Biology Centre CAS, Na Sádkách 7, 370 05 České

11 Budějovice, Czech Republic

12

13 Correspondence: Roey Angel (roey.angel@bc.cas.cz), Talia Gabay (taliamoann@gmail.com)

14



## 15 Abstract

16 Biological soil crusts (biocrusts) are key contributors to desert ecosystem functions; therefore,  
17 biocrust restoration following mechanical disturbance is imperative. In the Negev Desert  
18 hyperarid regions, phosphate mining has been practiced for over 60 years, destroying soil  
19 habitats, and fragmenting the landscape. To understand the effects of mining activity on soil  
20 health, we previously characterized the biocrust communities in four phosphate mining sites  
21 over spatial (post-mining and natural plots) and temporal (2-10 years since restoration) scales.  
22 We showed that bacterial abundance, richness, and diversity in natural plots were significantly  
23 higher than in post-mining plots, regardless of temporal scale. In this study, we selected one  
24 mining site and used DNA stable isotope probing (DNA-SIP) to identify which bacteria grow in  
25 post-mining and natural biocrusts. Since biocrust communities activate only after wetting, we  
26 incubated the biocrusts with  $\text{H}_2^{18}\text{O}$  for 96 hours under ambient conditions. We then evaluated  
27 the physicochemical soil properties, chlorophyll *a* concentrations, activation, and functional  
28 potential of the biocrusts. The DNA-SIP assay revealed low bacterial activity in both plot types  
29 and no significant differences in the proliferated communities' composition when comparing  
30 post-mining and natural biocrusts. We further found no significant differences in the microbial  
31 functional potential, photosynthetic rates, or soil properties. Our results suggest that growth  
32 of hyperarid biocrust bacteria after wetting is minimal. We hypothesize that due to the harsh  
33 climatic conditions, during wetting bacteria devote their meager resources to prepare for the  
34 coming drought, by focusing on damage repair, and organic compound synthesis and storage  
35 rather than on growth. These low growth rates contribute to the sluggish recovery of desert



36 biocrusts following major disturbances such as mining. Therefore, our findings highlight the  
37 need for implementing active restoration practices following mining.

38

### 39 **Keywords**

40 Biological soil crust; Biocrust restoration; Stable isotope probing; Hyperarid desert; Mining;  
41 Restoration

42

43



## 44 1. Introduction

45 Phosphate mining in the Negev Desert, Israel, has been taking place since the 1960s in large  
46 areas. ILC-Rotem mining company leads the phosphate mining activities and has been  
47 practicing a reclamation-oriented mining protocol for the past 15 years. The mining protocol  
48 entails the excavation of the top 50-70 cm of soil (which they consider to be topsoil) followed  
49 by the overburden (the layer covering the phosphate), then storing the two soil layers in  
50 separate piles. Following the excavation of the phosphate, the overburden is returned to the  
51 mining pit followed by the topsoil. Finally, the terrain is leveled with heavy machinery. The  
52 area is then considered a restored, post-mining site.

53

54 Open mining activities lead to the destruction of the local vegetation and seed bank, and the  
55 fragmentation of the natural landscape (Sengupta, 2021). The consequences include land  
56 degradation, erosion, soil and water pollution, and dust dispersion. In addition, mining  
57 activity often leads to decreased biodiversity in and around mining sites (Bridge, 2004,  
58 Sengupta, 2021). One of the ecosystem components being destroyed by mining activities in  
59 the Negev Desert is the biological soil crust layer (biocrust). Biocrust is the topmost layer of  
60 many arid soils and comprises primary-producing and heterotrophic microorganisms that  
61 bind together soil particles using secreted extracellular polymeric substances (EPS), mainly  
62 polysaccharides (Weber et al., 2022). Biocrusts provide many ecosystem services, including  
63 fixing nitrogen and carbon, and soil stabilization (Belnap and Lange, 2003). While biocrust  
64 microorganisms developed various adaptations to withstand the harsh desert environment



65 (Makhalanyane et al., 2015), biocrust structures are susceptible to mechanical disturbances.

66 Such a disturbance, especially over large scales (for example, mining activity), breaks and

67 buries biocrust organisms, often resulting in changed biocrust communities (Belnap and

68 Eldridge, 2003).

69

70 In a previous research, we evaluated the biocrust bacterial communities in phosphate

71 mining sites (Gabay et al., 2022). Briefly, we found that natural and post-mining biocrusts

72 differ in community composition and diversity. Following the biocrust community analysis,

73 we sought to identify which bacterial groups are actively growing in the biocrust and

74 whether the composition differs between natural and post-mining sites. To this end, we used

75 DNA-stable isotope probing (DNA-SIP): a culture-free approach that allows the detection of

76 actively growing microorganisms by labeling them with stable isotopes such as  $^{15}\text{N}$ ,  $^{14}\text{C}$ , and

77  $^{18}\text{O}$  (Dumont and Hernández García, 2019). SIP has been widely applied in identifying

78 microbial groups that participate in carbon and nitrogen cycling, such as methanotrophs

79 (Sultana et al., 2019, Zhang et al., 2020), methylotrophs (Macey et al., 2020, Arslan et al.,

80 2022), and nitrogen fixers (Pepe-Ranney et al., 2016, Angel et al., 2018). Likewise, SIP can use

81 the incorporation of heavy water ( $\text{H}_2^{18}\text{O}$ ) into various biomarkers to study the growth and

82 function of microorganisms that become activated upon wetting (Schwartz et al., 2019).

83 Previous  $\text{H}_2^{18}\text{O}$  SIP experiments measured microbial growth rates and dynamics following

84 hydration (Blazewicz et al., 2020). Desert biocrusts make an ideal study system for  $\text{H}_2^{18}\text{O}$  SIP

85 experiments, as they become active quickly following hydration (Angel and Conrad, 2013),



86 resuming growth, nutrient cycling, and excretion of extracellular organic materials (Garcia-

87 Pichel and Belnap, 1996, Belnap and Lange, 2003).

88

89 In this research, we investigated the proliferation of bacterial groups in biocrusts taken from

90 reference ('natural') areas and post-mining sites by incubating biocrust samples with

91 isotopically-labeled water ( $\text{H}_2^{18}\text{O}$ ). We hypothesized that growth patterns and taxonomic

92 identity of bacterial groups would differ significantly when comparing natural and post-

93 mining biocrusts. Specifically, we expected higher bacterial growth rates in natural

94 compared to post-mining biocrusts. Based on our previous findings, we specifically expected

95 higher activity of Cyanobacteria in the natural biocrusts (Gabay et al., 2022).



## 96 2. Materials and Methods

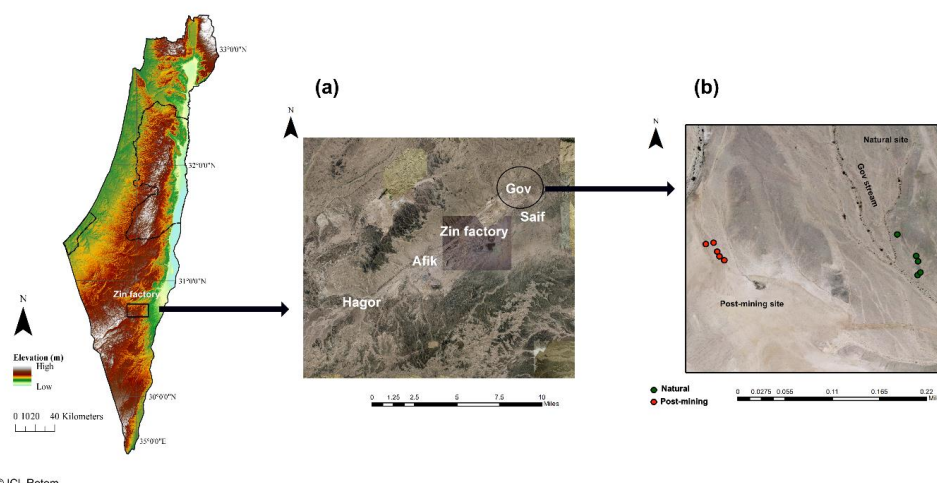
97

### 98 2.1. Study site and sample collection

99 Sampling was conducted during June 2020 at the Gov Mining Site, located in the Zin Valley  
100 (30.84 °N, 35.09 °E, 98 m above sea level), where restoration was completed in 2007. The study  
101 area was previously described in Gabay et al., (2022). Briefly, Zin Valley is a hyperarid region of  
102 the Negev Desert, with 50 mm average annual rainfall (Zin factory meteorological data). The  
103 soils are highly saline (average EC = 24 dS/m), composed of variable amounts of sand, silt, and  
104 clay, and are classified as Solonchaks according to the World Reference Based soil  
105 classification system.

106

107 Biocrusts were sampled either from the post-mining site or the adjacent natural area. In each  
108 sampling site, we sampled along a 100 m strip at approximately 10 m intervals (Fig. 1). In total,  
109 we sampled 20 biocrust samples (10 from each site). We collected the biocrusts using a  
110 spatula, at an average depth of 2 mm. Biocrusts were placed in 100 mm x 15 mm petri dishes  
111 lined with cotton. For the SIP assay, we chose 5 of the 10 samples from each site containing  
112 the highest chlorophyll *a* concentrations as estimated in preliminary experiments (Table S1).



113

114 Figure 1: map of the research area. Map a shows the different post-mining sites around the  
 115 Zin factory. Map b shows the biocrust sampling points in gov mining site used for this  
 116 research. Green dots represent the natural biocrusts, and red dots represent the post-mining  
 117 biocrusts.

118

119

## 120 2.2. Soil properties

121 Five biocrust samples from each plot type (post-mining and natural) were sent for analysis of  
 122 soil properties (pH, EC,  $\text{NO}_3^-$  concentrations, and soil organic matter). The analysis was  
 123 performed at the Gilat Soil Laboratory (Gilat Research Center, Gilat, Israel).

124

## 125 2.3. chlorophyll *a* extraction

126 Chlorophyll *a* was extracted from biocrust samples using a protocol previously described in  
 127 Gabay et al., (2022). Briefly, chlorophyll *a* was extracted from 3 g soil of each biocrust sample





128 was diluted in 9 mL of methanol for 15 min at 65 °C. The soil solution was centrifuged at 2000  
129 rpm for 5 minutes, supernatant was collected, and absorbance was measured in a  
130 spectrophotometer at 665 nm. Concentrations were calculated according to Ritchie (2006)  
131 and normalized to 1 g of soil. Extractions of the biocrusts were performed before (dry  
132 biocrusts) and after 96 hr incubation with distilled water (DW) under identical conditions to  
133 the incubation with H<sub>2</sub><sup>18</sup>O.

134

## 135 2.4. Stable isotope probing

### 136 2.4.1. Soil incubation

137 To test the incorporation of <sup>18</sup>O into biocrust samples, a microcosm was designed to control  
138 for the incubation conditions. Each microcosm consisted of a 10 mL glass vial in which 1 g of  
139 biocrust sample was placed. To achieve field water-holding capacity, 0.15 mL of H<sub>2</sub><sup>18</sup>O or  
140 DNase-free water were added. The glass vials were then sealed with butyl rubber stoppers  
141 (Sigma-Aldrich, St. Louis, Missouri, United States) to prevent evaporation. Both labeled and  
142 unlabeled controls were incubated in duplicates, for a total of 40 vials. Samples were  
143 incubated under a 12 hr photoperiod for 96 hr in an incubator (FOC 225 I, VELP Scientifica,  
144 Usmate Velate MB, Italy) to allow the incorporation of <sup>18</sup>O into the bacterial DNA. Following  
145 incubation, the microcosms were sacrificed, and each biocrust sample was divided into 4  
146 bead beating tubes (Qiagen, Hilden, Germany), each containing 0.25 g of soil, and stored at -  
147 80 °C until further analysis.



148 Each labeled sample had a non-labeled control, incubated under identical conditions but  
149 with DNase-free water instead of  $^{18}\text{O}$  water.

150

#### 151 **2.4.2. DNA extraction**

152 DNA was extracted from all biocrust samples using DNeasy PowerSoil Pro Kit (Qiagen),  
153 according to the manufacturer's instructions. The biomass in hyperarid biocrusts tends to be  
154 very low, yielding only minute amounts of DNA. Therefore, each 1 g soil was extracted in  
155 batches of 0.25 g, and the extracts were later consolidated to increase DNA yield.

156

#### 157 **2.4.3. SIP gradient preparation and fractionation**

158 DNA (ca. 3.5 ng) was subjected to isopycnic gradient centrifugation in a solution of caesium  
159 chloride (7.163 M; CsCl, Sigma Aldrich. St Loise, MI, USA) and buffer (0.1 M Tris-HCl at pH 8.0,  
160 0.1 M KCl and 1 mM EDTA, all from Sigma Aldrich) to a final density of  $1.725 \text{ g mL}^{-1}$  as described  
161 previously (Jia et al., 2019). The tubes were spun for 44 hr at 177,000 g and then fractionated  
162 by water displacement using a syringe pump (NE-300 Just Infusion™ Syringe Pump, NewEra  
163 Pump systems, Farmingdale, NY, USA). The refractive index was measured using an AR200  
164 digital refractometer (Reichert, Depew, NY, USA) and then the DNA was precipitated using a  
165 Polyethylene Glycol 6000 solution (30% PEG 8000 and 1.6 M NaCl), and 30  $\mu\text{g}$  of GlycoBlue  
166 Coprecipitant (Thermo Fisher Scientific, Waltham, MS, USA). Copy numbers of the 16S rRNA  
167 gene in each fraction were determined by qPCR using a probe-based approach. Primers 338F  
168 and 805R (Yu et al., 2005) coupled with a 516P probe (FAM-BHQ1 dual labeled) were used for



169 the assay. Per one reaction 10  $\mu$ L of TaqMan™ Fast Advanced Master Mix (Thermo Fisher  
170 Scientific), 4  $\mu$ L of Bovine Saline Albumin (BSA; Thermo Fisher Scientific), 1  $\mu$ L of each primer  
171 (10  $\mu$ M), 0.4  $\mu$ L of a probe (10  $\mu$ M) and 2.2  $\mu$ L of PCR water was combined and mixed with 5  $\mu$ L  
172 of DNA. After 5 min initial denaturation at 95 °C, cycling program: 40 cycles of 95 °C for 30 sec  
173 followed by 62 °C for 1 min was applied. Gene copy numbers were established from a standard  
174 curve of *Escherichia coli* 16S rRNA gene.

175

#### 176 2.4.4. PCR and sequencing

177 Following fractionation, all samples (labeled and unlabeled) were amplified using the 16S  
178 rRNA primers 515F\_mod and 806R\_mod (Apprill et al. 2015, Parada et al. 2016). Each reaction  
179 consisted of 2.5  $\mu$ L Green Taq Buffer (Thermo Fisher Scientific), 2.5  $\mu$ L of dNTP set  
180 (Biotech rabbit, Berlin, Germany), 0.1  $\mu$ L of BSA (Thermo Fisher Scientific), 0.625  $\mu$ L of each  
181 primer (10  $\mu$ M), 0.125  $\mu$ L DreamTaq Green DNA Polymerase (Thermo Fisher Scientific) and 17.5  
182  $\mu$ L of PCR water (Sigma). The PCR ran for 38 cycles using the following program: denaturation  
183 at 94 °C for 45 sec, annealing at 52 °C for 45 sec, extension at 72 °C for 45 sec, and a final cycle  
184 of extension at 72 °C for 10 min. The amplified fragments were sequenced using MiniSeq  
185 (Illumina, San Diego, CA, USA) at the UIC sequencing core, University of Illinois, Chicago, Illinois  
186 (<https://rrc.uic.edu/cores/genome-research/genome-research-core/>). DNA extraction and SIP  
187 gradient controls, PCR negative controls and mock community (ZymoBIOMICS Microbial  
188 Community Standard II Log Distribution; Zymo Research, Irvine, CA, USA) samples (2 of each)  
189 were also sequenced to control for contaminants in the sequencing results.



190

## 191 2.5. Bioinformatic analysis

192 All the bioinformatic and statistical analyses were done in R V4.1.1 (R development core  
193 team, 2013). Labeling of bacteria was detected using differential abundance analysis as  
194 described in Angel (2019). Briefly, the sequences were processed using the DADA2 package  
195 V8.8 (Callahan et al., 2016) for quality filtering, denoising, read-merging, chimera removal,  
196 constructing amplicon sequence variants (ASV) tables, and taxonomic assignment. Detection  
197 and removal of potential contaminant sequences were performed using the R package  
198 decontam V1.12.0 (Davis et al., 2017). Prevalence filtering of rare ASVs was done using the  
199 Phyloseq package V1.36.0 (McMurdie and Holmes, 2013). ASVs that appeared in less than  
200 2.5% of the samples were removed. A maximum-likelihood phylogenetic tree was calculated  
201 using IQ-TREE2 V 2.1.1. (Minh et al., 2020). Finally, differential abundance analysis was  
202 performed using DESeq2 V1.32.0 (Love et al., 2014) to compare the relative abundance of  
203 each ASV in the heavy fractions of labeled DNA to the unlabeled heavy fractions (the negative  
204 control samples), which allows identifying the bacterial groups that incorporated the water  
205 isotope into their DNA. The results were filtered to include only ASVs with a 2-fold log change  
206 and a significance value  $p < 0.1$ .

207

## 208 2.6. Predictions of genomic functions

209 Abundances of functional genes based on 16S rRNA gene abundances were performed using  
210 Picrust2 (Douglas et al., 2019). Abundances of functional genes were predicted based on a



211 filtered ASV table containing only ASVs belonging to proliferated bacteria based on the  
212 differential abundance modeling. The resulting output is functional identifications that were  
213 annotated using the KEGG database to infer functional gene families. Each gene was then  
214 classified into 10 function categories based on Meier et al. (2021). The abundance of genes  
215 within each category was averaged.

216

## 217 **2.7. Statistical analyses**

218 chlorophyll *a* concentrations were visualized as an estimation plot using the dabestr  
219 package V0.3.0 (Ho and Tumkaya, 2018). The effect size was calculated as a bootstrap 95%  
220 confidence interval. Abundances of functional genes and soil properties were compared  
221 between natural and post-mining biocrusts using Mann-Whitney tests. The community  
222 composition of natural and post-mining biocrusts was assessed using only sequences  
223 belonging to proliferated bacteria based on DESeq2 modeling. The weighted UniFrac  
224 (Lozupone et al., 2011) was used to calculate the similarity between the natural and post-  
225 mining communities, and an adonis model was used to assess whether communities differ  
226 significantly from each other (package Vegan V2.6-2; Dixon, 2003).

227

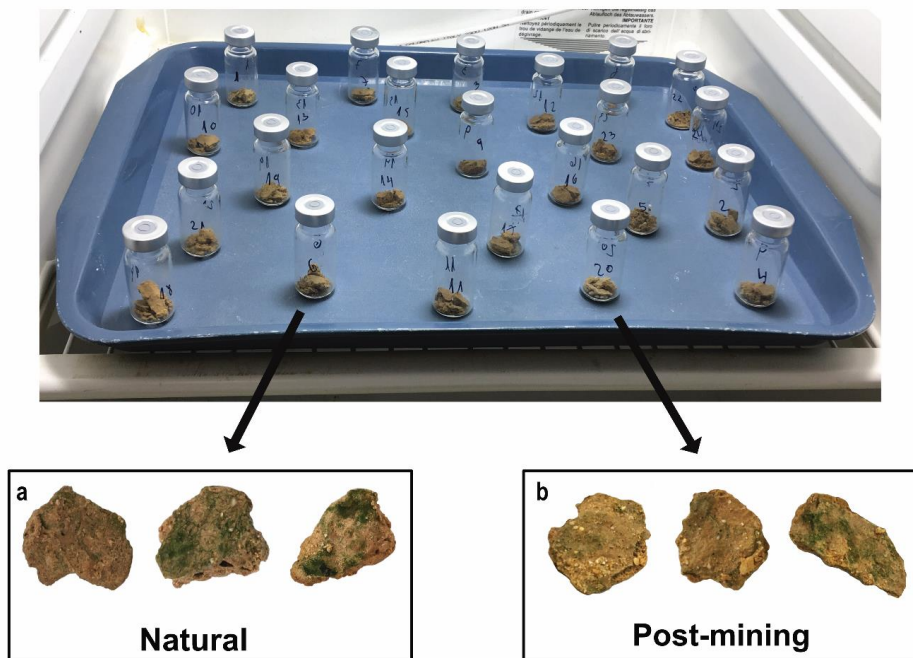


## 228 3. Results

### 229 Sample wetting and greening

230 Most biocrust samples (both natural and post-mining) showed greening within 36 to 48 hr  
231 into the 96 hr incubation. By the end, most samples displayed varying degrees of greening,  
232 indicating cyanobacterial activity. Generally, post-mining biocrust showed less greening than  
233 the natural biocrusts (Fig. 2).

234



235

236

237 Figure 2: Incubation setup. Top picture – biocrusts in sealed glass vials in the incubator.  
238 Bottom picture – natural (a) and post-mining (b) biocrusts following the 96-hour incubation.

239



## 240 Soil properties

241 EC and  $\text{NO}_3^-$  were significantly higher in natural biocrusts compared to post-mining biocrusts  
 242 (EC:  $t = 2.89$ ,  $p < 0.05$ ;  $\text{NO}_3^-$ :  $t = 4$ ,  $p < 0.01$ ; Table 1). Soil organic matter was also significantly  
 243 higher in the natural biocrusts ( $t = 3.77$ ,  $p < 0.01$ ; Table 1). pH was slightly higher in natural  
 244 biocrusts; however, the differences were not statistically significant (pH:  $t = 1.41$ ,  $p = 0.19$ ;  
 245 Table 1).

246

247 Table 1: soil properties for natural and post-mining biocrusts. The numbers represent the  
 248 means for each property. Significant differences are marked with an asterisk (\* =  $p < 0.05$ ; \*\* =  
 249  $p < 0.01$ ).

250

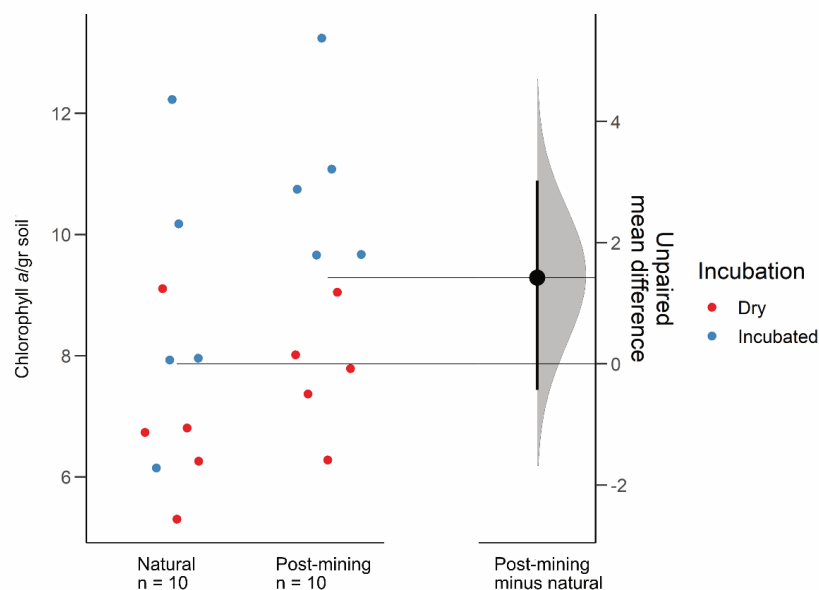
Plot type/Soil property	Natural	Post-mining
pH	7.6	7.5
EC	26.22*	9.94
$\text{NO}_3^-$	84.82**	14.75
Soil organic matter	1.2**	0.81

251

252

## 253 Chlorophyll *a*

254 The estimation plot revealed an effect size estimate at 1.42 (95CI -0.432; 3.03; Fig. 3). In the  
 255 natural samples, there was no clear clustering according to the soil water content i.e., dry or  
 256 hydrated (following 96 hr incubation with water). In fact, there was a larger variance between  
 257 samples collected after incubation (Fig. 3). Hydrated post-mining biocrusts had consistently  
 258 higher chlorophyll *a* concentrations compared to dry biocrusts. It is also apparent that the  
 259 variance between samples was smaller in the post-mining biocrusts (Fig. 3).



260

261 Figure 3: Estimation plots of chlorophyll a concentrations. Dots represent the biocrust  
262 samples, and colors represent either dry or incubated soil.

263

## 264 Sequencing and differential abundance modeling

265 Sequencing resulted in 47,311 reads per sample on average (Table S2) and 10,275 ASVs

266 (Table S3). Following decontamination and filtering, 86% of the ASVs were removed (Table

267 S3). However, they accounted for only 16% of the total reads. Out of the remaining 1,404

268 ASVs, 1266 in total were labeled and used for the differential abundance modeling (Table S3).

269 Each sequence in the labeled samples was compared to its corresponding negative control,

270 and the Log<sub>2</sub>-fold change in labeled sequences was evaluated to determine whether an ASV

271 could be considered truly labeled (i.e., belonging to growing bacteria) based on the

272 significance threshold. One of the natural biocrust samples (no. 1; Fig. 4) displayed much

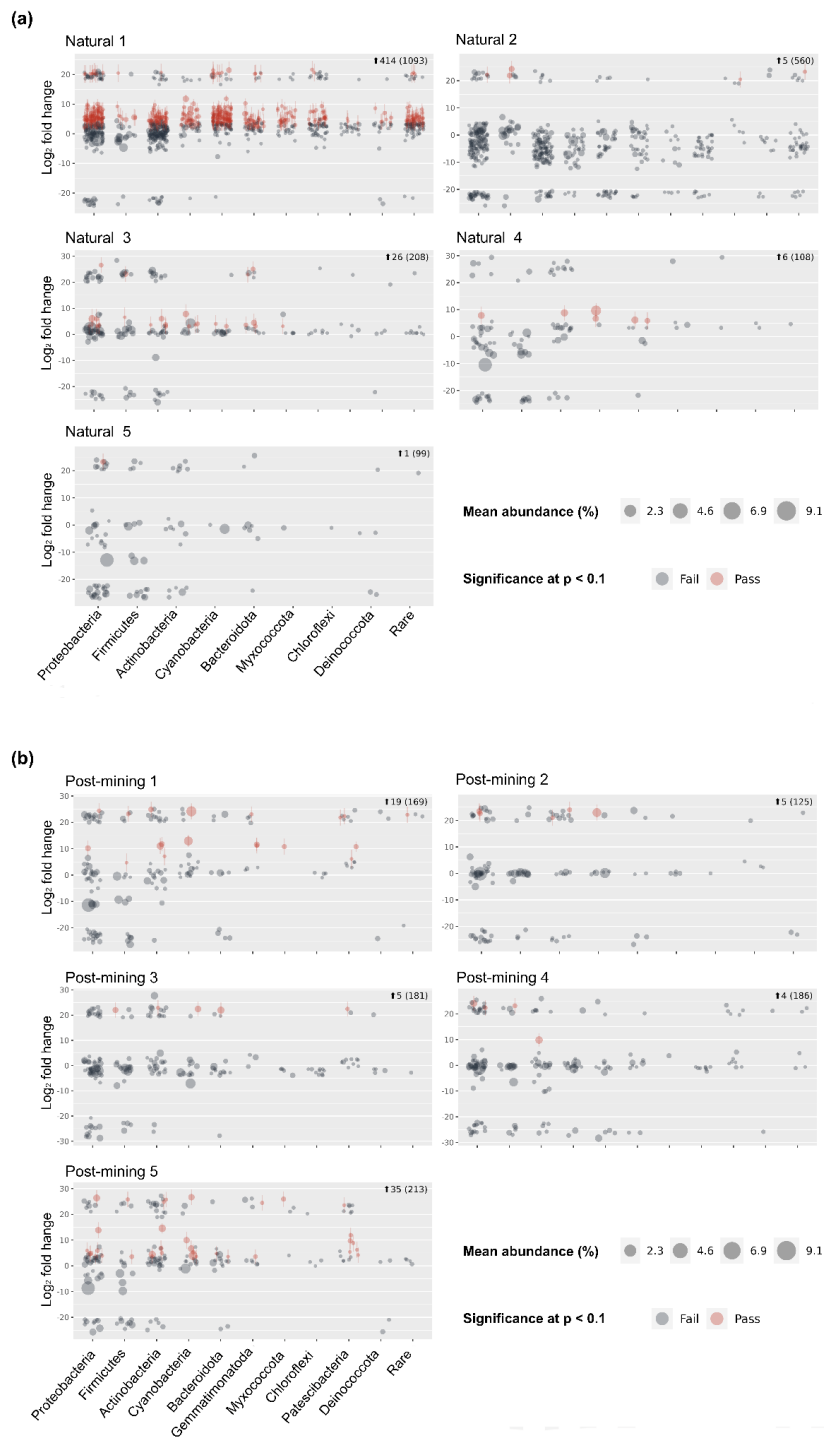
273 higher labeling than the other 4 samples (414 ASVs passed, out of a total of 1,093; Fig. 4).





274 Excluding sample 1, 38 out of 975 ASVs total passed the significance threshold for Log<sub>2</sub> fold  
275 change. In post-mining samples, the number of labeled reads was more consistent among  
276 the different samples (Fig. 4). 68 ASVs out of 874 ASVs total passed the threshold for Log<sub>2</sub> fold  
277 change. Altogether, the number of labeled ASVs did not differ significantly between natural  
278 and post-mining samples (natural sample 1 was excluded, natural community mean = 9.5,  
279 post-mining community mean = 13.6, W= 9, p = 0.9).

280



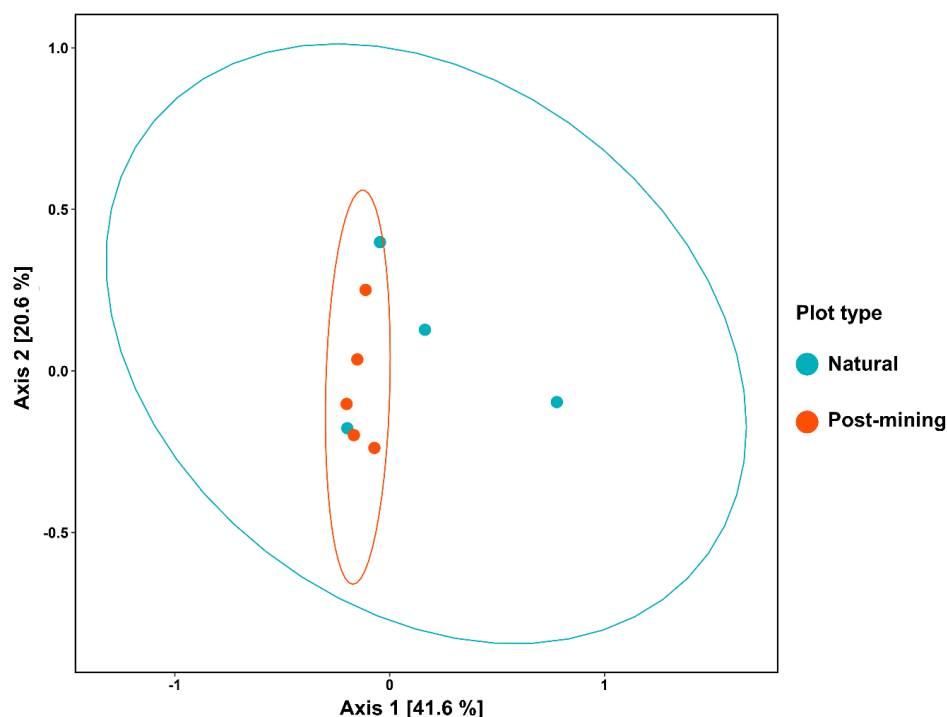


282 Figure 4: community composition of proliferated bacteria in natural (a) and post-mining (b)  
283 biocrusts. Each graph represents a different sample. Red dots indicate labeled ASVs, and  
284 grey dots indicate unlabeled ASVs, based on Deseq2 modeling.

285

## 286 Composition of the proliferated bacterial community

287 Figure 5 depicts PCoA ordination based on weighted UniFrac metric showing that the  
288 biocrust samples do not cluster according to plot type (natural sample 1 was excluded).  
289 Furthermore, the adonis test revealed no significant differences in community composition  
290 (Weighted UniFrac ~ Plot type;  $F = 1.23$ ,  $R^2 = 0.15$ ,  $p = 0.21$ ). Phylogenetic trees depict the  
291 different bacterial groups indicating that, for the most part, sequences that appear in natural  
292 and post-mining biocrusts belong to the same orders/classes. In the phylum Cyanobacteria,  
293 labeled sequences belonged to two classes, and most sequences in both natural and post-  
294 mining samples belonged to the class Cyanobacteria, with a slightly higher prevalence in the  
295 post-mining samples (Fig. S1). The class Bacteroidia, belonging to the phylum Bacteroidota,  
296 had a similar prevalence for natural and post-mining samples (Fig. S1). The trend was similar  
297 in the class Bacilli, belonging to the phylum Firmicutes (Fig. S1). In the Alphaproteobacteria  
298 phylum, the orders Rhodobacterales, Rhizobiales and Sphingomonadales appeared in both  
299 natural and post-mining samples (Fig. S1). The phylum Gammaproteobacteria appeared  
300 only once in post-mining samples but was more prevalent in natural samples (Fig. S1). The  
301 phylum Actinobacteria was more prevalent in post-mining samples, yet the orders  
302 Frankiales, Micrococcales and Propionibacteriales appeared in both natural and post-mining  
303 samples (Fig. S1). A Venn diagram of unique and overlapping sequences reveals that only 8  
304 out of 88 labeled sequences appear both in natural and post-mining samples (Fig. S2).



305

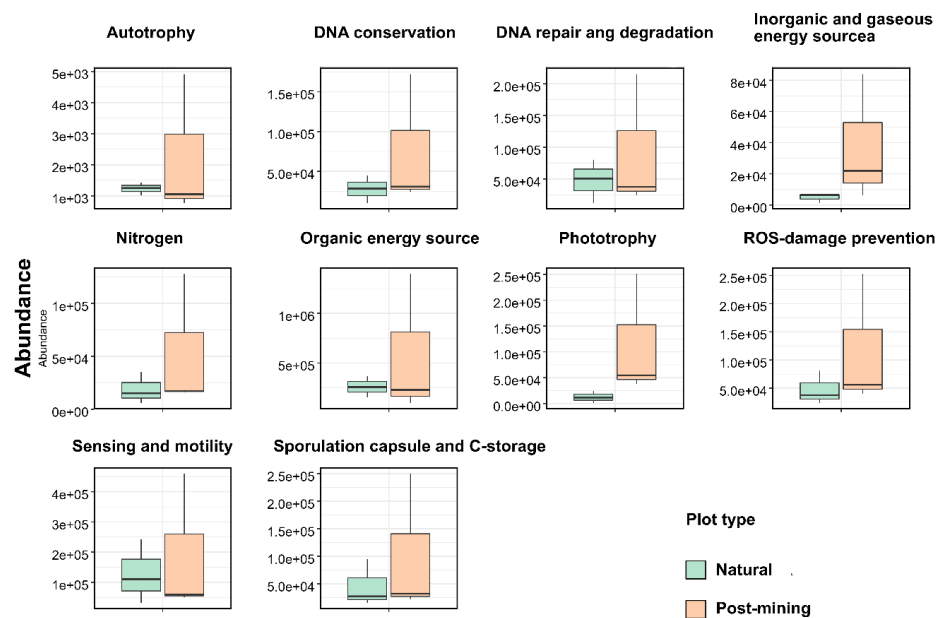
306 Figure 5: PCoA ordination of community composition based on weighted UniFrac similarity  
307 metric. Blue dots are natural samples and pink dots are post-mining samples. The ellipses  
308 represent 95% confidence intervals.

309

### 310 Predictions of genomic functions

311 Abundances of 10 function categories (listed in Table S4) were compared between natural  
312 and post-mining biocrust samples. Abundances were generally higher in post-mining  
313 compared to natural biocrusts (Table S4). Also, the variance between samples was larger in  
314 post-mining biocrust (Fig. 6). However, the differences between plot types were not  
315 statistically significant in any of the function categories (Fig. 6, Table S4).

316



317  
318 Figure 6: boxplot of functional predictions. The Y axis represents functional gene  
319 abundances. The line represents the median, and the whiskers represent the range.  
320  
321



## 322 Discussion

323 In this study, we examined which groups of the biocrust bacterial communities grow after  
324 hydration using a SIP assay and differential abundance modelling. We hydrated and  
325 incubated the biocrusts for 96 hr expecting bacterial growth, yet very little growth was  
326 detected. Only 3.9% of the natural and 7.7% of the post-mining biocrusts' ASVs were  
327 identified as truly labeled by the stable isotope. Post-mining biocrusts had a slightly higher  
328 number of labeled ASVs compared to natural biocrusts but, the differences were not  
329 significant. Also, the composition and taxonomic identity of the growing communities did  
330 not significantly differ between natural and post-mining biocrusts.

331

332 Biocrust organisms are known to resume activity quickly following hydration, resuming  
333 functions such as damage repair, germination, nutrient cycling, and growth (Harel et al.,  
334 2004, Rajeev et al., 2013, Green and Proctor, 2016, Thomas et al., 2022). Hydration may also  
335 lead to changes in biocrust bacterial communities (Angel and Conrad, 2013; Štovíček and  
336 Gillor, 2022). In a  $\text{H}_2^{18}\text{O}$  SIP assay using the Negev Desert biocrusts from arid and hyperarid  
337 regions, samples were hydrated and incubated for three weeks at maximum water holding  
338 capacity. Within days, changes in the labeled bacterial community composition and  
339 abundance were observed, indicating growth (Angel and Conrad, 2013). Similarly, biocrusts  
340 collected in the Negev Desert during a rain event and subsequent desiccation, demonstrated  
341 an increase in Cyanobacteria and decrease in Actinobacteria abundance (Baubin et al.,  
342 2021), implying selective proliferation of bacterial taxa in the hydrated biocrust.



343 In other H<sub>2</sub><sup>18</sup>O SIP assays on soil bacterial communities, a quick response to re-wetting was  
344 observed, and bacterial growth was evident within 24 to 72 hours of incubation (Blazewicz et  
345 al., 2014, Aanderud et al., 2015). Thus, we assumed that hydration and incubation of  
346 hyperarid biocrusts under favorable conditions would result in growth. We expected distinct  
347 proliferated communities when comparing natural and post-mining biocrusts, given our  
348 previous results that demonstrated that the bacterial community differed between natural  
349 and post-mining biocrusts (Gabay et al., 2022).

350

351 Our previous survey of biocrust bacterial communities in the Zin mining area revealed  
352 significantly lower abundances of cyanobacteria and chlorophyll *a* concentrations (Gabay et  
353 al., 2022). Out of the four mining sites surveyed, Gov (which was restored in 2007) showed the  
354 most considerable shift in biocrust community following mining. However, in the current  
355 study, we sampled post-mining biocrusts at a different location (~500 m away from the  
356 original plot) due to technical constraints. In the new location we found that the  
357 photosynthetic potential in the post-mining biocrust did not differ from the natural biocrust.  
358 These results highlight the importance of microenvironments in shaping the functionality of  
359 biocrusts (Garcia-Pichel and Belnap, 1996). The similarities in active communities and  
360 photosynthetic potential could be due to more developed biocrusts in the new sampling  
361 location compared to the previous ones.

362



363    Photosynthetic activity is usually observed in biocrusts within minutes to hours after  
364    hydration by either dew or rain (Harel et al., 2004; Lange, 2003). In our experiment, we  
365    hydrated the biocrusts to capacity and then incubated the samples for 96 hr. During the  
366    incubation, most biocrust samples displayed some degree of greening, with more greening  
367    in the natural biocrusts (Fig. 2). This indicates that the photosynthetic bacteria in the  
368    biocrust were activated upon wetting. Yet, no significant differences were detected between  
369    natural and post-mining biocrusts, chlorophyll *a* concentrations (Fig. 3) or functional  
370    predictions (Fig. 6). This implies that similar abundances of photosynthetic bacteria were  
371    activated upon wetting in both biocrusts, yet, they barely proliferated (Fig. 4).

372

373    The growth patterns of biocrust organisms are affected by local environmental conditions  
374    (Kim and Or, 2017). Zin mining fields are in an hyperarid region, where extreme heat events  
375    are frequent in the summer, and rains are scarce and unpredicted. Moreover, in recent years  
376    there were only two or three rain events during each rainy season (Zin factory meteorological  
377    data). Hydration is the most important factor affecting biocrust organisms' growth rate while  
378    long desiccation periods negatively affect growth (Zaady et al., 2016). Also, salinity levels in  
379    Zin valley soils are high (Table 1; Levi et al., 2021). We suggest that due to these conditions,  
380    the hyperarid biocrust communities prioritize activation and preparation for desiccation  
381    over growth. It is known that in high stress environments, biocrust microorganisms resume  
382    carbon and nitrogen fixation upon hydration. The resulting organic carbon and nitrogen  
383    compounds can be metabolized during the long desiccation periods (Belnap, 2003; Colesie  
384    et al., 2014).





385 Natural recovery of biocrusts has been long debated, and is generally estimated to be a slow  
386 process, especially in sites that experience very short activity times for biocrust  
387 development, such as the hyperarid Zin mining site (Kidron et al., 2020; Weber et al., 2016).  
388 The time and trajectory of recovery depend on many factors relating to local climatic  
389 conditions and site properties (Belnap and Lange, 2003). One such factor that greatly affects  
390 establishment and restoration of biocrusts is the proximity, availability, and dispersal timing  
391 of biocrust propagules (Bowker, 2007, Walker et al., 2007). Thus, the low proliferation rates  
392 we observed, particularly in post-mining biocrusts, suggest that restoration processes might  
393 be much slower than previously estimated. The topsoil from a stockpile is used to cover the  
394 mining pits. This soil may not contain a rich biocrust seed bank that was probably destroyed  
395 and buried during the mining processes. Further increase in bacterial biomass might highly  
396 depend on the dispersal of biocrust propagules to the site from adjacent natural areas by  
397 wind or water. Our results further emphasize the need for active restoration measures in Zin  
398 mines. Such measures include soil inoculation with local cyanobacterial propagules (Acea,  
399 2003, Wang et al., 2009, Zhao et al., 2016, Velasco Ayuso et al., 2017) and increased hydration  
400 (Morillas & Gallardo, 2015, Zhang et al., 2018), which are effective methods in enhancing  
401 biocrust establishment and recovery following disturbances (Antoninka et al., 2020).

402

403



## 404 Conclusions

405 Low proliferation of biocrust bacteria was detected after wetting suggesting prolonged  
406 recovery times of biocrusts following major mechanical disturbance, such as mining.  
407 Furthermore, recovery largely depends on site conditions and the ability of biocrust  
408 propagules to disperse to post-mining sites. Further research is needed to confirm our  
409 hypothesis of low proliferation and thus restoration rates in hyperarid biocrust bacterial  
410 communities.

411

## 412 Code and data availability

413 All data produced in this study and scripts used for community analysis, functional  
414 predictions and chlorophyll *a* estimation plot are available at  
415 <https://github.com/TaliaJoanne/SIP-experiment-Zin-mines>.

416 The raw 16S sequences are available in the NCBI database under Bioproject ID  
417 PRJNA906925, accession numbers SAMN31937891 – SAMN31937900.

418

## 419 Author's contributions

420 Talia Gabay: Conception, Sample Collection, Incubation, Chlorophyll *a* and DNA extraction,  
421 Statistical Analysis, Visualization, Writing-Original Draft Preparation, Writing-Reviewing and  
422 Editing. Eva Petrova: DNA-SIP assay, DNA quantification and PCR amplification. Osnat Gillor  
423 and Yaron Ziv: Conception, Writing-Reviewing and Editing, Investigation, Supervision. Roey



424 Angel: Conception, Statistical Analysis, Visualization, Supervision, Writing-Reviewing and  
425 Editing.

426 All authors read and approved the manuscript.

427

#### 428 **Declaration of competing interest**

429 The authors declare that they have no known competing financial interests or personal  
430 relationships that could have appeared to influence the work reported in this paper.

431

#### 432 **Acknowledgements**

433 We thank Matan Avital from ICL for coordinating sample collection and providing Zin factory  
434 maps and meteorological data, Sharon Moscovitz for her assistance in sample collection and  
435 Ofer Ovadia for suggestions on statistical analyses. Lastly, we thank ICL Rotem LTD for their  
436 support and funding of this research.

437

#### 438 **Financial support**

439 Funding for this research was provided by Rotem ICL LTD. RA was supported by the Czech  
440 Science Foundation (Junior Grant No. 19-24309Y), EP was supported by the Czech Ministry of  
441 Education Youth and Sport (EF16\_013/0001782 - SoWa Ecosystems Research).

442



## References

- Aanderud, Z. T., Jones, S. E., Fierer, N., and Lennon, J. T.: Resuscitation of the rare biosphere contributes to pulses of ecosystem activity, *Front. Microbiol.*, 6, <https://doi.org/10.3389/fmicb.2015.00024>, 2015.
- Angel, R.: Stable Isotope Probing Techniques and Methodological Considerations Using  $^{15}\text{N}$ , in: *Stable Isotope Probing: Methods and Protocols*, edited by: Dumont, M. G. and Hernández García, M., Springer New York, New York, NY, 175–187, [https://doi.org/10.1007/978-1-4939-9721-3\\_14](https://doi.org/10.1007/978-1-4939-9721-3_14), 2019.
- Angel, R. and Conrad, R.: Elucidating the microbial resuscitation cascade in biological soil crusts following a simulated rain event: Microbial resuscitation in biological soil crusts, *Environ Microbiol.*, n/a–n/a, <https://doi.org/10.1111/1462-2920.12140>, 2013.
- Angel, R., Panhölzl, C., Gabriel, R., Herbold, C., Wanek, W., Richter, A., Eichorst, S. A., and Wobken, D.: Application of stable-isotope labelling techniques for the detection of active diazotrophs: Detecting diazotrophs with stable-isotope techniques, *Environ Microbiol.*, 20, 44–61, <https://doi.org/10.1111/1462-2920.13954>, 2018.
- Anon: Dabestr: Data Analysis Using Bootstrap-Coupled Estimation, 2020.
- Antoninka, A., Faist, A., Rodriguez-Caballero, E., Young, K. E., Chaudhary, V. B., Condon, L. A., and Pyke, D. A.: Biological soil crusts in ecological restoration: emerging research and perspectives, *Restor Ecol.*, 28, <https://doi.org/10.1111/rec.13201>, 2020.
- Arslan, M., Müller, J. A., and Gamal El-Din, M.: Aerobic naphthenic acid-degrading bacteria in petroleum-coke improve oil sands process water remediation in biofilters: DNA-stable isotope probing reveals methylotrophy in Schmutzdecke, *Science of The Total Environment*, 815, 151961, <https://doi.org/10.1016/j.scitotenv.2021.151961>, 2022.
- Baubin, C., Ran, N., Siebner, H., and Gillor, O.: The response of desert biocrust bacterial communities to hydration-desiccation cycles, *SOIL Discussions*, 1–48, 2021.
- Belnap, J.: The world at your feet: desert biological soil crusts, *Frontiers in Ecology and the Environment*, 1, 181–189, [https://doi.org/10.1890/1540-9295\(2003\)001\[0181:TWAYFD\]2.0.CO;2](https://doi.org/10.1890/1540-9295(2003)001[0181:TWAYFD]2.0.CO;2), 2003.
- Belnap, J. and Eldridge, D.: Disturbance and Recovery of Biological Soil Crusts, in: *Biological Soil Crusts: Structure, Function, and Management*, edited by: Belnap, J. and Lange, O. L., Springer Berlin Heidelberg, Berlin, Heidelberg, 363–383, [https://doi.org/10.1007/978-3-642-56475-8\\_27](https://doi.org/10.1007/978-3-642-56475-8_27), 2003.
- Belnap, J. and Lange, O. L. (Eds.) Baldwin, I. T., Caldwell, M. M., Heldmaier, G., Lange, O. L., Mooney, H. A., Schulze, E.-D., and Sommer, U.: *Biological Soil Crusts: Structure, Function, and Management*, Springer Berlin Heidelberg, Berlin, Heidelberg, <https://doi.org/10.1007/978-3-642-56475-8>, 2003.
- Blazewicz, S. J., Schwartz, E., and Firestone, M. K.: Growth and death of bacteria and fungi underlie rainfall-induced carbon dioxide pulses from seasonally dried soil, *Ecology*, 95, 1162–1172, <https://doi.org/10.1890/13-1031.1>, 2014.
- Blazewicz, S. J., Hungate, B. A., Koch, B. J., Nuccio, E. E., Morrissey, E., Brodie, E. L., Schwartz, E., Pett-Ridge, J., and Firestone, M. K.: Taxon-specific microbial growth and mortality patterns reveal distinct temporal population responses to rewetting in a California grassland soil, *ISME J.*, 14, 1520–1532, <https://doi.org/10.1038/s41396-020-0617-3>, 2020.
- Bridge, G.: CONTESTED TERRAIN: Mining and the Environment, *Annu. Rev. Environ. Resour.*, 29, 205–259, <https://doi.org/10.1146/annurev.energy.28.011503.163434>, 2004.
- Callahan, B. J., McMurdie, P. J., Rosen, M. J., Han, A. W., Johnson, A. J. A., and Holmes, S. P.: DADA2: High-resolution sample inference from Illumina amplicon data, *Nat Methods*, 13, 581–583, <https://doi.org/10.1038/nmeth.3869>, 2016.
- Colesie, C., Allan Green, T. G., Haferkamp, I., and Büdel, B.: Habitat stress initiates changes in composition,  $\text{CO}_2$  gas exchange and C-allocation as life traits in biological soil crusts, *ISME J.*, 8, 2104–2115, <https://doi.org/10.1038/ismej.2014.47>, 2014.
- Davis, N. M., Proctor, D., Holmes, S. P., Relman, D. A., and Callahan, B. J.: Simple statistical identification and removal of contaminant sequences in marker-gene and metagenomics data, *bioRxiv*, 221499, <https://doi.org/10.1101/221499>, 2017.
- Dixon, P.: VEGAN, a package of R functions for community ecology, *Journal of Vegetation Science*, 14, 927–930, <https://doi.org/10.1111/j.1654-1103.2003.tb02228.x>, 2003.



- 493 Douglas, G. M., Maffei, V. J., Zaneveld, J., Yurgel, S. N., Brown, J. R., Taylor, C. M., Huttenhower, C., and Langille, M.  
494 G. I.: PICRUSt2: An improved and customizable approach for metagenome inference, *Bioinformatics*,  
495 <https://doi.org/10.1101/672295>, 2019.
- 496 Dumont, M. G. and Hernández García, M. (Eds.): *Stable Isotope Probing: Methods and Protocols*, Springer New  
497 York, New York, NY, <https://doi.org/10.1007/978-1-4939-9721-3>, 2019.
- 498 Gabay, T., Rotem, G., Gillor, O., and Ziv, Y.: Understanding changes in biocrust communities following phosphate  
499 mining in the Negev Desert, *Environmental Research*, 207, 112200,  
500 <https://doi.org/10.1016/j.envres.2021.112200>, 2022.
- 501 Garcia-Pichel, F. and Belnap, J.: Microenvironments and Microscale Productivity of Cyanobacterial Desert Crusts,  
502 *J Phycol*, 32, 774–782, <https://doi.org/10.1111/j.0022-3646.1996.00774.x>, 1996.
- 503 Green, T. G. A. and Proctor, M. C. F.: Physiology of Photosynthetic Organisms Within Biological Soil Crusts: Their  
504 Adaptation, Flexibility, and Plasticity, in: *Biological Soil Crusts: An Organizing Principle in Drylands*, edited  
505 by: Weber, B., Büdel, B., and Belnap, J., Springer International Publishing, Cham, 347–381,  
506 [https://doi.org/10.1007/978-3-319-30214-0\\_18](https://doi.org/10.1007/978-3-319-30214-0_18), 2016.
- 507 Harel, Y., Ohad, I., and Kaplan, A.: Activation of Photosynthesis and Resistance to Photoinhibition in  
508 Cyanobacteria within Biological Desert Crust, *Plant Physiology*, 136, 3070–3079,  
509 <https://doi.org/10.1104/pp.104.047712>, 2004.
- 510 Jia, Z., Cao, W., and Hernández García, M.: DNA-based stable isotope probing, in: *Stable Isotope Probing*,  
511 Springer, 17–29, 2019.
- 512 Kidron, G. J., Xiao, B., and Benenson, I.: Data variability or paradigm shift? Slow versus fast recovery of biological  
513 soil crusts—a review, *Science of The Total Environment*, 721, 137683,  
514 <https://doi.org/10.1016/j.scitotenv.2020.137683>, 2020.
- 515 Kim, M. and Or, D.: Hydration status and diurnal trophic interactions shape microbial community function in  
516 desert biocrusts, *Biogeosciences*, 14, 5403–5424, <https://doi.org/10.5194/bg-14-5403-2017>, 2017.
- 517 Lange, O. L.: Photosynthesis of Soil-Crust Biota as Dependent on Environmental Factors, in: *Biological Soil*  
518 *Crusts: Structure, Function, and Management*, edited by: Belnap, J. and Lange, O. L., Springer Berlin  
519 Heidelberg, Berlin, Heidelberg, 217–240, [https://doi.org/10.1007/978-3-642-56475-8\\_18](https://doi.org/10.1007/978-3-642-56475-8_18), 2003.
- 520 Levi, N., Hillel, N., Zaady, E., Rotem, G., Ziv, Y., Karnieli, A., and Paz-Kagan, T.: Soil quality index for assessing  
521 phosphate mining restoration in a hyper-arid environment, *Ecological Indicators*, 125, 107571,  
522 <https://doi.org/10.1016/j.ecolind.2021.107571>, 2021.
- 523 Love, M. I., Huber, W., and Anders, S.: Moderated estimation of fold change and dispersion for RNA-seq data with  
524 DESeq2, *Genome Biol*, 15, 550, <https://doi.org/10.1186/s13059-014-0550-8>, 2014.
- 525 Lozupone, C., Lladser, M. E., Knights, D., Stombaugh, J., and Knight, R.: UniFrac: an effective distance metric for  
526 microbial community comparison, *The ISME journal*, 5, 169–172, 2011.
- 527 Macey, M. C., Pratscher, J., Crombie, A. T., and Murrell, J. C.: Impact of plants on the diversity and activity of  
528 methylotrophs in soil, *Microbiome*, 8, 31, <https://doi.org/10.1186/s40168-020-00801-4>, 2020.
- 529 Makhalanyane, T. P., Valverde, A., Gunnigle, E., Frossard, A., Ramond, J.-B., and Cowan, D. A.: Microbial ecology of  
530 hot desert edaphic systems, *FEMS Microbiology Reviews*, 39, 203–221,  
531 <https://doi.org/10.1093/femsre/fuu011>, 2015.
- 532 McMurdie, P. J. and Holmes, S.: phyloseq: An R Package for Reproducible Interactive Analysis and Graphics of  
533 Microbiome Census Data, *PLOS ONE*, 8, e61217, <https://doi.org/10.1371/journal.pone.0061217>, 2013.
- 534 Meier, D. V., Imminger, S., Gillor, O., and Woebken, D.: Distribution of Mixotrophy and Desiccation Survival  
535 Mechanisms across Microbial Genomes in an Arid Biological Soil Crust Community, *mSystems*, 6, e00786-  
536 20, <https://doi.org/10.1128/mSystems.00786-20>, 2021.
- 537 Minh, B. Q., Schmidt, H. A., Chernomor, O., Schrempf, D., Woodhams, M. D., von Haeseler, A., and Lanfear, R.: IQ-  
538 TREE 2: New Models and Efficient Methods for Phylogenetic Inference in the Genomic Era, *Molecular*  
539 *Biology and Evolution*, 37, 1530–1534, <https://doi.org/10.1093/molbev/msaa015>, 2020.
- 540 Pepe-Ranney, C., Koehler, C., Potrafka, R., Andam, C., Eggleston, E., Garcia-Pichel, F., and Buckley, D. H.: Non-  
541 cyanobacterial diazotrophs mediate dinitrogen fixation in biological soil crusts during early crust  
542 formation, *ISME J*, 10, 287–298, <https://doi.org/10.1038/ismej.2015.106>, 2016.
- 543 Rajeev, L., da Rocha, U. N., Klitgord, N., Luning, E. G., Fortney, J., Axen, S. D., Shih, P. M., Bouskill, N. J., Bowen, B.  
544 P., Kerfeld, C. A., Garcia-Pichel, F., Brodie, E. L., Northen, T. R., and Mukhopadhyay, A.: Dynamic



- 545 cyanobacterial response to hydration and dehydration in a desert biological soil crust, *ISME J*, 7, 2178–
- 546 2191, <https://doi.org/10.1038/ismej.2013.83>, 2013.
- 547 Schwartz, E., Hayer, M., Hungate, B. A., and Mau, R. L.: Stable Isotope Probing of Microorganisms in
- 548 Environmental Samples with H<sub>2</sub> 18 O, in: *Stable Isotope Probing*, Springer, 129–136, 2019.
- 549 Sengupta, M.: Environmental impacts of mining: monitoring, restoration, and control, Second edition., CRC
- 550 Press, Boca Raton, FL ; Abingdon, Oxon, 1 pp., 2021.
- 551 Štovíček, A. and Gillor, O.: The Response of Soil Microbial Communities to Hydration and Desiccation Cycles in
- 552 Hot Desert Ecosystems, in: *Microbiology of Hot Deserts*, edited by: Ramond, J.-B. and Cowan, D. A.,
- 553 Springer International Publishing, Cham, 319–339, [https://doi.org/10.1007/978-3-030-98415-1\\_11](https://doi.org/10.1007/978-3-030-98415-1_11), 2022.
- 554 Sultana, N., Zhao, J., Zheng, Y., Cai, Y., Faheem, M., Peng, X., Wang, W., and Jia, Z.: Stable isotope probing of
- 555 active methane oxidizers in rice field soils from cold regions, *Biol Fertil Soils*, 55, 243–250,
- 556 <https://doi.org/10.1007/s00374-018-01334-7>, 2019.
- 557 Team, R. C.: R: A language and environment for statistical computing, 2013.
- 558 Thomas, A. D., Elliott, D. R., Hardcastle, D., Strong, C. L., Bullard, J., Webster, R., and Lan, S.: Soil biocrusts affect
- 559 metabolic response to hydration on dunes in west Queensland, Australia, *Geoderma*, 405, 115464,
- 560 <https://doi.org/10.1016/j.geoderma.2021.115464>, 2022.
- 561 Weber, B., Büdel, B., and Belnap, J. (Eds.): *Biological Soil Crusts: An Organizing Principle in Drylands*, Springer
- 562 International Publishing, Cham, <https://doi.org/10.1007/978-3-319-30214-0>, 2016.
- 563 Weber, B., Belnap, J., Büdel, B., Antoninka, A. J., Barger, N. N., Chaudhary, V. B., Darrouzet-Nardi, A., Eldridge, D.
- 564 J., Faist, A. M., Ferrenberg, S., Havrilla, C. A., Huber-Sannwald, E., Malam Issa, O., Maestre, F. T., Reed, S. C.,
- 565 Rodríguez-Caballero, E., Tucker, C., Young, K. E., Zhang, Y., Zhao, Y., Zhou, X., and Bowker, M. A.: What is a
- 566 biocrust? A refined, contemporary definition for a broadening research community, *Biological Reviews*,
- 567 97, 1768–1785, <https://doi.org/10.1111/brv.12862>, 2022.
- 568 Yu, Y., Lee, C., Kim, J., and Hwang, S.: Group-specific primer and probe sets to detect methanogenic communities
- 569 using quantitative real-time polymerase chain reaction, *Biotechnology and bioengineering*, 89, 670–679,
- 570 2005.
- 571 Zaady, E., Eldridge, D. J., and Bowker, M. A.: Effects of Local-Scale Disturbance on Biocrusts, in: *Biological Soil*
- 572 *Crusts: An Organizing Principle in Drylands*, edited by: Weber, B., Büdel, B., and Belnap, J., Springer
- 573 International Publishing, Cham, 429–449, [https://doi.org/10.1007/978-3-319-30214-0\\_21](https://doi.org/10.1007/978-3-319-30214-0_21), 2016.
- 574 Zhang, L., Dumont, M. G., Bodelier, P. L. E., Adams, J. M., He, D., and Chu, H.: DNA stable-isotope probing
- 575 highlights the effects of temperature on functionally active methanotrophs in natural wetlands, *Soil*
- 576 *Biology and Biochemistry*, 149, 107954, <https://doi.org/10.1016/j.soilbio.2020.107954>, 2020.
- 577
- 578